Volume 253, number 1,2, 231–234 FEB 07483 August 1989

Diameter of the mitochondrial outer membrane channel: evidence from electron microscopy of frozen-hydrated membrane crystals

Carmen A. Mannella, Xiao-Wei Guo and Bernard Cognon

Wadsworth Center for Laboratories and Research, New York State Department of Health, Empire State Plaza, Albany, NY 12201 and Departments of Physics and Biomedical Sciences, State University of New York at Albany, Albany, NY, USA

Received 10 May 1989

The average projected density of mitochondrial outer membrane channels has been obtained from electron microscopic images of unstained, frozen-hydrated two-dimensional crystals. The density map is consistent with the projection of hollow, thin-walled cylinders aligned normal to the membrane plane with a diameter of 3.8 ± 0.1 nm. This diameter closely matches that of the largest β-barrel that can be formed from one copy of the 30-kDa mitochondrial outer membrane channel protein.

Mitochondrial outer membrane; Ion channel; Electron microscopy; (*Neurospora crassa*)

1. INTRODUCTION

The permeability of the mitochondrial outer membrane to metabolites and ions has been attributed to the presence of numerous channels formed by one or more copies of a 30-kDa polypeptide, representing as much as 1% of the total mitochondrial protein mass [1–3]. This channel has been named VDAC for voltage-dependent, anion-selective channel. When reconstituted in phospholipid bilayers, it forms a large pore (unit conductance of 4.5 nS in 1 M KCl) which is somewhat more permeable to anions than to cations and which switches to lower conductance substates with applied transmembrane potential [1,2].

We have used techniques of negative-stain electron microscopy and computer image processing to study the structure of the mitochondrial outer membrane channel. These studies have been made possible by the discovery that the channels spontaneously crystallize in the plane of the outer membrane of *Neurospora* mitochondria by the action of soluble phospholipase A_2 [4]. In the normally observed parallelogram VDAC array, six channels occupy the unit cell (fig.1A). Little or no protein protrudes from the membrane surface, so that the main features in projection images of negatively stained VDAC crystals are the dense, stain-filled circular lumens of the pores [5].

In order to obtain direct information about the protein which forms the VDAC pore, we have turned to electron microscopic imaging of unstained, frozen-hydrated VDAC arrays. This technique, which has seen widespread application in recent years, involves freezing the specimen at liquid-nitrogen temperature in a thin layer of water at a rate sufficiently rapid so that non-crystalline or vitreous ice is formed [6,7]. Such specimens can be examined in the electron microscope by employing special cryotransfer devices and protocols to minimize irradiation of the specimens (which are considerably more sensitive to electron beam damage than equivalent specimens stained with heavy metal salts). Because of the absence of stain, contrast in projection images of such specimens arises solely from inherent density differences among the membrane components, i.e. protein,

Correspondence address: C.A. Mannella, Wadsworth Center for Laboratories and Research, New York State Department of Health, Empire State Plaza, Albany, NY 12201, USA

Published by Elsevier Science Publishers B.V. (Biomedical Division)
00145793/89/$3.50

lipid and water, projected across the thickness of the array.

2. METHODS

Crystalline arrays of mitochondrial outer membrane channels were prepared from *Neurospora crassa* as previously described [4,5]. Specimens of membrane crystals were deposited on carbon-coated Cu grids, blotted and rapidly plunged into liquid ethane in thermal contact with liquid nitrogen. These frozen-hydrated specimens were transferred to and examined in a Philips EM420 electron microscope using a Gatan model 626 cryotransfer device. Images were recorded under minimal-dose conditions [5] at 100 kV, using a defocus of −250 to −500 nm. Image averages were obtained by correlation analysis [8,9] a technique which involves precisely locating and summing the unit cells in a given crystal field. Image processing was performed as described in detail elsewhere [5], using the SPIDER image processing system [10].

For comparison between observed projection averages and models, the phase residual criterion [11] was used. The phase residual is defined as:

$$\Delta\phi = \left(\frac{\sum_R (|M_1| + |M_2|)(\Delta\theta)^2}{\sum_R (|M_1| + |M_2|)} \right)^{1/2}$$

where $\Delta\theta$ is the phase difference between the complex Fourier coefficients of two images, M_1 and M_2, and the summations are made over an annulus, R, in Fourier space. For the calculations of table 1, the annulus radii (1/5.0–1/2.0 nm^{-1}) were chosen to include the strongest maxima in the frozen-hydrated image transform (see section 3 and fig.1C). For these calculations, a soft (Gaussian fall-off) circular mask was applied around the central unit cell in the images.

3. RESULTS AND DISCUSSION

The projection image of an unstained, frozen-hydrated VDAC array, obtained by correlation averaging, is presented as fig.1B. Each of the six channel positions in the unit cell has a central white (low density) core bounded by a dark (high density) rim. This is the expected projected density profile for a water-filled lumen enclosed by a cylindrical protein wall. On the outside of the hexameric groups of channels are low-density regions which generally correlate with sites of light staining by uranyl acetate, fig.1A, suggesting that they represent phospholipid domains [5]. In addition, 'arms' of high density (protein) extend between channels of adjacent unit cells (arrow in fig.1B).

Fourier transforms of correlation averages like those of fig.1B contain weak maxima out to 1/1.0 nm^{-1} (fig.1C). However, most of the intensity in these spectra is contained within the first six diffraction orders, so that the effective resolution in these correlation averages is about 1/2.0 nm^{-1}. Clearly, higher resolution projection averages are needed before direct determination of the secondary structure of the VDAC channel protein is possible. However, the available projected density map is sufficient for basic model testing.

We have modeled the VDAC channel as a simple hollow cylinder normal to the membrane plane by placing a narrow ring of unit density (against a zero-density background) at each of the positions occupied by the channels in the VDAC array (fig.1D). Ring diameters were varied systematically from 2.5 to 5.0 nm and phase residuals (see section 2) were calculated between these models and the correlation average of fig.1B. A phase residual of 45° or less is conventionally taken to indicate satisfactory agreement between two images. As indicated in table 1, agreement was found between model and data over a very limited range of ring diameter: 3.8 ± 0.1 nm. Fig.1E is the projection of the model consisting of 3.8 nm-diameter hollow cylinders low-pass filtered to 1/2.0 nm^{-1}, the effective resolution of the frozen-hydrated VDAC density map in fig.1B. Note that several (but not all) of the modulations in the channel rims are duplicated in the two projections. Also, the dense arms at the corners of the unit cells in the average of fig.1B are not reproduced by low-pass filtration of the model.

While the 'minimal' model of fig.1D may be refined in several ways, the basic agreement between it and the observed projection data is very striking. Forte et al. [12] have noted that the VDAC sequence contains a prominent pattern of alternating polar and nonpolar residues, appropriate for an anti-parallel β-barrel structure. Polar residues would point into the aqueous lumen while the nonpolar amino acids would face outwards to interact with the hydrophobic interior of the bilayer. A β-barrel consisting of a 3.8 nm-diameter α-carbon cylinder, with a 0.5 nm-thick 'shell' of amino acid residues on either side, would be consistent with several other known or inferred physical characteristics of VDAC. The inner diameter of such a β-barrel, 2.8 nm, correlates well with values based on negative stain exclusion from the channel lumens, 2.5 to 3.0 nm [5]. This inner diameter also falls in the middle of the range

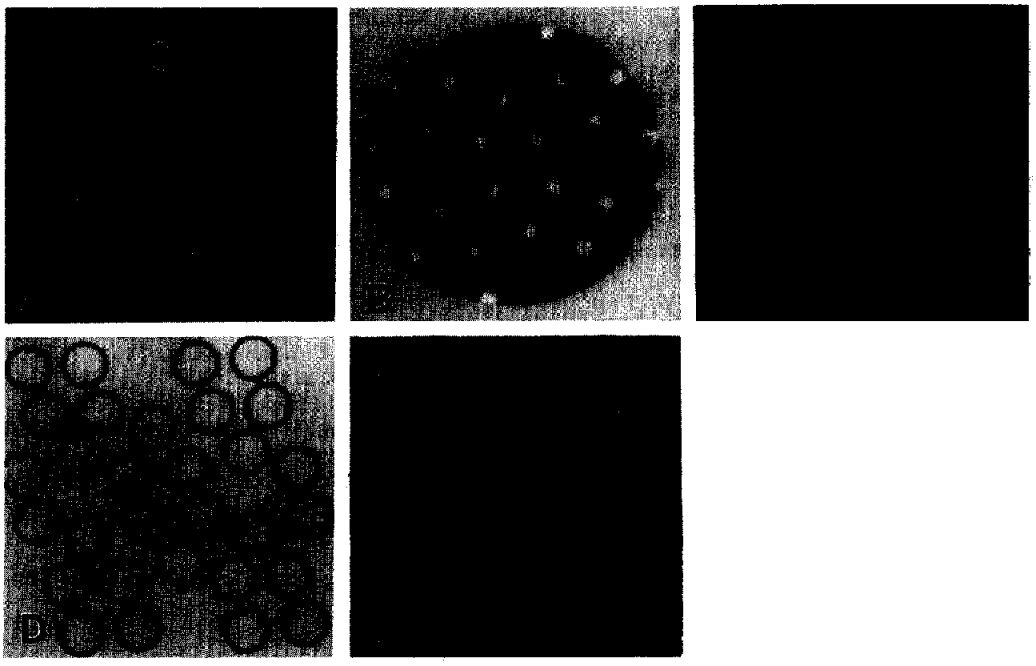

Fig.1. (A,B) Correlation averages of *Neurospora* VDAC array embedded in uranyl acetate (A) and vitreous ice (B). The average in (A) is summed over several thousand unit cells, that in (B) over 220 unit cells. The cell vectors (a = 13 nm, b = 11.5 nm) are indicated in (A). Note that the lumens are dark (stain-filled) in the negatively stained specimen and white (water-filled) in the frozen-hydrated specimen. (C) Transform of the correlation average in (B). The white ring indicates a radius of 1/2.0 nm^{-1}; amplitudes outside this radius are enhanced by a factor of 5. The arrow and arrowhead indicate reflections at 1/1.2 nm^{-1}, and 1/1.05 nm^{-1}, respectively. (D) Model array composed of rings 0.3 nm wide and 3.8 nm in diameter, positioned at the coordinates of the channels in the VDAC array. (E) The model in (D) low-pass filtered to 1/2.0 nm^{-1}.

predicted on the basis of permeability characteristics of the VDAC channel, 1.7–4.0 nm [3,13]. Likewise, the outer barrel diameter, 4.8 nm, is consistent with the center-to-center distances observed between adjacent channels in the array, 4.5–5.5 nm. It is also within the range of the channel outer-diameter inferred from X-ray scattering experiments with plant mitochondrial outer membranes, 4–5 nm [14].

Table 1

Phase residual agreement between the observed projection density for crystalline VDAC and cylinder models of varying diameter

Cylinder diameter (nm)	Phase residual (deg)
3.2	78
3.5	59
3.7	43
3.8	34
3.9	45
4.2	69
4.4	86

Forte et al. [12] postulated that the VDAC channel might be formed by a single copy of the 30-kDa outer mitochondrial membrane polypeptide. They noted that the widest transmembrane β-barrel into which the VDAC sequence can be folded contains 19 β-strands ('staves'), using all of the sequence except for 21 residues at the amino-terminus which may form an amphipathic helix [15]. This hypothetical 'monomer' barrel would have a carbon-backbone diameter of 3.8 nm if the β-chains were tilted 38° relative to the long axis of the barrel, very close to the energetically optimal tilt angle of 36° (Guy, H.R., personal communication). Thus, although there is biochemical and functional evidence that favors a 'dimer' VDAC channel [1,16], a monomer channel cannot presently be eliminated on the basis of existing structural data.

Acknowledgements: This material is based on work supported by grant DMB-8613702 from the National Science Foundation. The authors thank Drs Joachim Frank, H. Robert Guy and Marco Colombini for helpful discussions on this manuscript.

REFERENCES

[1] Colombini, M. (1986) in: Ion Channel Reconstitution (Miller, C. ed.) pp.533–552, Plenum, NY.
[2] Freitag, H., Neupert, W. and Benz, R. (1982) Eur. J. Biochem. 123, 629–639.
[3] De Pinto, V., Ludwig, O., Krause, J., Benz, R. and Palmieri, F. (1987) Biochim. Biophys. Acta 894, 109–119.
[4] Mannella, C.A. (1984) Science 224, 165–166.
[5] Mannella, C.A., Ribeiro, A. and Frank, J. (1986) Biophys. J. 49, 307–318.
[6] Taylor, K.A. and Glaeser, R.M. (1976) J. Ultrastruct. Res. 55, 448–456.
[7] Adrian, M., Dubochet, J., Lepault, J. and McDowall, A. (1984) Nature 308, 32–36.
[8] Saxton, W.O. (1980) in: Electron Microscopy at Molecular Dimensions (Baumeister, W. and Vogell, W. eds) pp.244–255, Springer, Berlin.
[9] Frank, J. (1982) Optik 63, 67–89.
[10] Frank, J., Shimkin, B. and Dowse, H. (1981) Ultramicroscopy 6, 343–358.
[11] Frank, J., Verschoor, A. and Boublik, M. (1981) Science 214, 1353–1355.
[12] Forte, M., Guy, H.R. and Mannella, C.A. (1987) J. Bioenerget. Biomembr. 19, 341–350.
[13] Colombini, M. (1980) J. Membr. Biol. 53, 79–84.
[14] Mannella, C.A. and Bonner, W.D., jr (1975) Biochim. Biophys. Acta 413, 226–233.
[15] Kleene, R., Pfanner, N., Pfaller, R., Link, T.A., Sebald, W., Neupert, W. and Tropschug, M. (1987) EMBO J. 6, 2627–2633.
[16] Linden, M. and Gellerfors, P. (1983) Biochim. Biophys. Acta 736, 125–129.